

Contact Phase Invariant Control for Humanoid Robot based on Variable Impedant Inverted Pendulum Model

Tomomichi Sugihara[†], Yoshihiko Nakamura^{†,††}

[†] Dept. of Mechano-Informatics, Univ. of Tokyo.
7-3-1, Hongo, Bunkyo-ku, Tokyo, 113-8656, Japan.
E-mail: sugihara@ynl.t.u-tokyo.ac.jp

^{††} Japan Science and Technology Corporation(JST), CREST Program.

Abstract

Being expected as the utilities in the future, humanoid robots should be given much higher mobility. A seamless transition between contact and aerial phase is essential to behave robustly against disturbance in the real environment, and to expand the range of their activities and perform a variety of motion. Manipulation of both the contact condition and the external force is the key issue to enhance the mobility of humanoids since they are driven by the external force converted from the inner force through the interaction with the environment. The difficulty lies on the complexity of their dynamics so that they consist of a number of degrees of freedom and their structures vary in accordance with contact phase transition. We propose Variable Impedant Inverted Pendulum(VIIP) model control which allows one to handle the external force rather easily. The advantage of the proposed is that it is invariant on contact phase so that both cases in contact and in aerial are treated in the unified way. It also reduces the amount of computation. Thus, quick responsive motion of the robot can be practically achieved. We verified the effect of the controller in computer simulation, using a small humanoid robot model.

1 Introduction

Humanoid robots have much potential to become superior utilities in the future. Having similar shapes to human-beings, they are expected to act wherever humans can act. Humanoids in presence, however, disappointingly lack of capability to perform flexibly in the real environment. Although not a few studies in this field have improved the mobility of legged machines [1, 2, 3, 4, 5, 6, 7], they have mainly focused on steady walking motion which assumes continuous contact with the ground at all. In order to put them into practical use in severe circumstances, they should be given much more enhanced mobility. Especially, a seamless transition between contact phase and aerial phase is required i) to cope with emergency in the case that robots suffer from large impacts, or ii) to expand the range of their activities and perform a variety of motion.

Some previous researches have achieved typical types of motion which go through aerial phase such as jumping and running with legged machines. Raibert et al.[8] realized hopping motion and even somersault with simple body robots by combination of simple controlling methods. It is not promising for humanoid robots as dynamically complex systems. Nagasaka[9], Yamane et al.[10] and Kajita et al.[11] developed pattern generation methods of jumping and running for humanoids. Motion planning and control, however, are inseparable in nature since humanoid is dominated by non-holonomic constraints in accordance with the presence of underactuated links. Hirano et al.[12] studied jumping motion of a humanoid robot in computer simulation using an adaptive impedance control. It is for achievement of repeating jumping. Mita et al.[13] proposed Variable Constraint Control. Though it is effective against non-holonomic constraint, an explicit representation of equation of motion of the robot is needed. And thus, the more complicated the system is, the more amount of computation it requires. It is necessary for quick responsive motion to make the amount of computation less and the control period short. Arikawa et al.[14] developed a Multi-DOF jumping Robot and controlled it according to pre-planned polynomial trajectories. It is not robust against disturbance. Pfeiffer et al.[15] are developing Jogging JOHN-NIE, aiming at fast movement through running. It is still under development.

The difficulty lies on the complexity of dynamics of humanoid robots. They consist of a number of links. And moreover, they have no fixed point in the inertia frame, which means that they are driven by the external reaction force, converting the inner force through the interaction with the environment. Manipulation of the external force, therefore, is the key issue to spread out the potential mobility of them. However, it generally suffers from the problem of time consumption for calculation.

The authors[16] had proposed the controlling method of humanoid robots through the indirect manipulation of ZMP [17], which is the point of action of the total external force. It equivalently enables to handle horizontal

components of the external force rather in a small amount of computation. Thanks to it, quick responsive motion and robust absorption of unpredicted impact have been achieved. In this paper, we augment it to realize a seamless transition between contact and aerial phase. The requirement for more positive manipulation of the external force is accomplished with Variable Impedant Inverted Pendulum(VIIP) model control.

The whole-body cooperative motion is created through the resolution of referential velocity into each joint motion synergetically. In this procedure, manipulation of the external force is treated just as a part of the constraints which determine the configuration of the robot. Consequently, the controller is contact phase invariant.

2 Variable Impedant Inverted Pendulum(VIIP) Model Control

2.1 VIIP Model

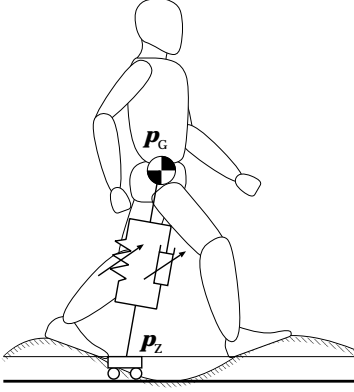


Figure 1: Legged system and VIIP model

When in contact phase, the robot can convert the inner force generated at each joint actuator to the external reaction force through the interaction with the environment. VIIP model functions during this phase to control the center of gravity(COG) effectively.

Suppose z -axis coincides with vertical direction, \mathbf{n}_Z is the total moment around ZMP, and $\mathbf{f}_G = [f_x \ f_y \ f_z]^T$, $\mathbf{n}_G = [n_x \ n_y \ n_z]^T$ are the force and moment acting at the center of gravity(COG). In accordance with both the equation of motion and the equilibrium of moment, we get the following equations.

$$m(\ddot{\mathbf{p}}_G + \mathbf{g}) = \mathbf{f}_G \quad (1)$$

$$(\mathbf{p}_G - \mathbf{p}_Z) \times \mathbf{f}_G + \mathbf{n}_G = \mathbf{n}_Z \quad (2)$$

where $\mathbf{g} = [0 \ 0 \ g]^T$ is the acceleration of gravity, and $\mathbf{p}_G = [x_G \ y_G \ z_G]^T$, $\mathbf{p}_Z = [x_Z \ y_Z \ z_Z]^T$ are the position of COG, ZMP respectively. Since the horizontal

components of \mathbf{n}_Z are zero by definition of ZMP,

$$\ddot{x}_G = \omega_G^2(x_G - x_Z) - \frac{n_y}{m(z_G - z_Z)} \quad (3)$$

$$\ddot{y}_G = \omega_G^2(y_G - y_Z) + \frac{n_x}{m(z_G - z_Z)} \quad (4)$$

$$\ddot{z}_G = \frac{f_z}{m} - g \quad (5)$$

where m is a total mass of the robot and ω_G is defined by

$$\omega_G^2 = \frac{f_z}{m(z_G - z_Z)} \quad (6)$$

One can associate Eq.(3)(4) with the dynamics of inverted pendulum although it has offset due to the existence of \mathbf{n}_G . Variation of \mathbf{n}_G under the influence of the whole-body motion is so less than that of \mathbf{f}_G in general that it can be neglected. Thus, \mathbf{n}_G can be regarded as a constant value in a short term. Consequently, the horizontal components of COG can be controlled through manipulation of ZMP as is already shown in [16].

Here, we focus on Eq.(5), which denotes the COG motion in vertical direction. Since the robot is unfixed on the ground, f_z must satisfy the following constraint.

$$f_z \geq 0 \quad (7)$$

When f_z equals to zero, the robot is in aerial phase, while f_z is greater than zero, the robot is in contact. It means that manipulation of f_z plays an important role for the seamless contact phase transition. Detachment off the ground requires large f_z to accelerate COG enough against gravity. Or, at the moment of touch down, f_z should be given compliance characteristic in order to absorb the impact. VIIP model shown in Fig.1 is that to realize such responsive and flexible motion in the unified way.

Based on the model, ${}^{ref}f_z$ is decided as

$${}^{ref}f_z = m\{K_{Pz}({}^{ref}z_G - z_G) + K_{Dz}({}^{ref}\dot{z}_G - \dot{z}_G) + g\} \quad (8)$$

where ${}^{ref}z_G$ is the referential COG in z -axis, whose meaning varies depending on the cases as is mentioned later. Substituting this ${}^{ref}f_z$ for f_z in Eq.(5), we get

$$\ddot{z}_G = K_{Pz}({}^{ref}z_G - z_G) + K_{Dz}({}^{ref}\dot{z}_G - \dot{z}_G) \quad (9)$$

2.2 Variable Design of Impedance

K_{Pz} and K_{Dz} in Eq.(9) should be chosen properly in accordance with the contact state and the motion scheme as is shown in Fig.2. I, II and III in Fig.2 are described as follows.

I) Impedance for lift-off

In addition to the acceleration of COG against gravity, velocity control is also essential to reach the desired height,

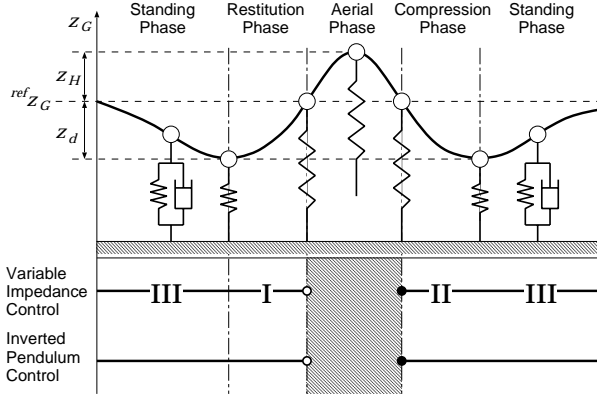


Figure 2: Contact phase, impedance and inverted pendulum control

since the initial velocity determines the maximum height in aerial phase. A simple spring model helps to meet this requirement. Suppose the robot lifts off when z_G equals to ${}^{ref}z_G$, the planned maximum jumping height from ${}^{ref}z_G$ in aerial phase is z_H , and stooping depth from ${}^{ref}z_G$ is z_d . In order to give the maximum vertical speed to the robot at the moment of detachment off, one should set K_{Dz} zero.

$$K_{Dz} = 0 \quad (10)$$

Then, we get the following equation from conservation of physical energy.

$$\frac{1}{2}mK_{Pz}z_d^2 = mgz_H \iff K_{Pz} = \frac{2gz_H}{z_d^2} \quad (11)$$

II) Impedance for touchdown

The spring model is also applicable for shock absorption at the touchdown. Suppose the robot lands onto the ground at the height ${}^{ref}z_G$ with falling speed immediately before contact \dot{z}_{G-} , and the desired maximum stooping depth from ${}^{ref}z_G$ is z_d . The impact at the touchdown is ideally eliminated if K_{Dz} is equal to zero. Then, we get

$$\frac{1}{2}m\dot{z}_d^2 = \frac{1}{2}mK_{Pz}z_d^2 \iff K_{Pz} = \left(\frac{\dot{z}_{G-}}{z_d}\right)^2 \quad (12)$$

which is also derived from conservation of physical energy.

III) Impedance in standing phase

Since Eq.(9) represents a second-order-lag system if both K_{Pz} and K_{Dz} are positive. Characteristic frequency and damping coefficient are

$$\omega = \sqrt{K_{Pz}}, \quad \zeta = \frac{K_{Dz}}{2\sqrt{K_{Pz}}} \quad (13)$$

For instance, z_G converges to ${}^{ref}z_G$ without overshoot when K_{Pz} and K_{Dz} satisfy the following condition.

$$\zeta > 1 \iff K_{Dz}^2 - 4K_{Pz} > 0 \quad (14)$$

In standing phase, however, f_z must satisfy the following condition to remain contact with the ground.

$${}^{ref}f_z > 0 \quad (15)$$

Thus, one should limit ${}^{ref}f_z$ to an appropriate minimum value ${}^{ref}f_{z,min} (> 0)$.

2.3 Indirect Manipulation of ZMP and Vertical Reaction Force

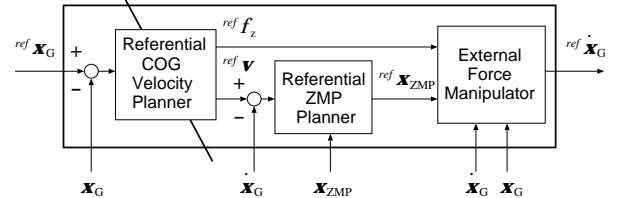


Figure 3: The external force manipulator

Though the dynamics of legged system is similar to that of inverted pendulum, it is impossible to manipulate ZMP and vertical reaction force directly. Therefore, the equivalent inner force to manipulate them indirectly should be obtained.

When the acceleration ${}^{ref}\ddot{\mathbf{p}}_G$ in (16)(17)(18) is given to COG instantaneously, ZMP and vertical reaction force coincide with ${}^{ref}\mathbf{p}_Z$ and ${}^{ref}f_z$ respectively, in accordance with the equations (3)(4)(5).

$${}^{ref}\ddot{x}_G = {}^{ref}\omega_G^2(x_G - {}^{ref}x_Z) - \frac{n_y}{m(z_G - {}^{ref}z_Z)} \quad (16)$$

$${}^{ref}\ddot{y}_G = {}^{ref}\omega_G^2(y_G - {}^{ref}y_Z) + \frac{n_x}{m(z_G - {}^{ref}z_Z)} \quad (17)$$

$${}^{ref}\ddot{z}_G = \frac{{}^{ref}f_z}{m} - g \quad (18)$$

where ${}^{ref}\ddot{\mathbf{p}}_G = [{}^{ref}\ddot{x}_G \quad {}^{ref}\ddot{y}_G \quad {}^{ref}\ddot{z}_G]^T$, and ${}^{ref}\omega_G$ is defined by

$${}^{ref}\omega_G^2 = \frac{{}^{ref}f_z}{m(z_G - {}^{ref}z_Z)} \quad (19)$$

and n_x, n_y are the current moment around x -axis, y -axis respectively. It requires a large amount of computation to calculate the equivalent inner force to the above acceleration exactly. Here, we integrate them and obtain the instantaneous strict referential velocity(SRV) of COG ${}^{ref}\dot{\mathbf{p}}_G$. COG Jacobian[16] \mathbf{J}_G (refer to the appendix, too) can relate ${}^{ref}\dot{\mathbf{p}}_G$ to the referential motion of the whole joints ${}^{ref}\dot{\boldsymbol{\theta}}$ ($n \times 1$, n : number of the robot joints) as follows.

$$\mathbf{J}_G {}^{ref}\dot{\boldsymbol{\theta}} = {}^{ref}\dot{\mathbf{p}}_G \quad (20)$$

Fig.3 figures a block diagram of the manipulator. Inserting this equation as a constraint to the whole-body cooperative motion control described in the next section, proper set of joint torque is calculated.

Although it is a pragmatic approach, ignoring the inertial force other than the gravitation, it can significantly reduce the amount of computation so that it helps realizing realtime implementation.

3 Contact Phase Invariant Whole-body Control based on SRV Resolution

Although the humanoid has tens of joints and thus is apparently complicated, the combination of various types of constraints due to contact with the environment or motion scheme itself determines large part of the configuration of the robot. This idea has a similar aspect with what is so-called *synergetics* in biological field. Biological system in general consists of an extremely large number of muscles as active elements, so that the management of them seems quite challenging. However, natural ingenious mechanism – connection with bones and tendons, internal coupling of joints, contact with the environment, and so forth – functions as the constraint and reduces the actual degrees of freedom of the system. Then, the skillful whole-body cooperation is achieved as the result.

All constraints can be classified into those originated either in physical law or in controlling scheme. Suppose motion commands such as motion of arm or foot step are given by a set of strict referential velocity, represented in the following form.

$$\mathbf{J}^{ref} \dot{\boldsymbol{\theta}} = {}^{ref} \mathbf{v} \quad (21)$$

Eq.(21) can be regarded as a sort of constraint for control. In this sense, Eq.(20) is no more than a part of the constraints.

Physically achievable constraints must be selected in accordance with the contact condition. For instance, motion of the system is strongly constrained by conservation of momentum and angular momentum due to the absence of external input while in aerial phase. Therefore, COG is uncontrollable and Eq.(20) is invalidated in this phase. The attitude and posture should be controlled instead, since they largely affects on the stability after landing as some former studies[8] revealed.

Now the problem is how to resolve ${}^{ref} \mathbf{v}$ into motion of the whole joints. We translate it into the following quadratic programming.

$$\begin{aligned} & \frac{1}{2} {}^{ref} \dot{\boldsymbol{\theta}}^T \mathbf{W} {}^{ref} \dot{\boldsymbol{\theta}} \longrightarrow \min. \\ & \text{subject to } \mathbf{J}^{ref} \dot{\boldsymbol{\theta}} = {}^{ref} \mathbf{v} \end{aligned} \quad (22)$$

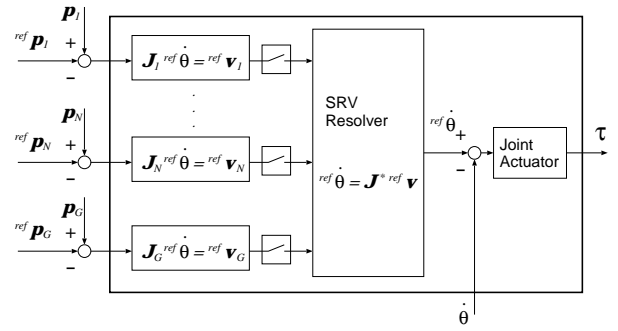


Figure 4: Procedure of SRV Resolution

and the solution is

$${}^{ref} \dot{\boldsymbol{\theta}} = \mathbf{W}^{-1} \mathbf{J}^T (\mathbf{J} \mathbf{W}^{-1} \mathbf{J}^T)^{-1} {}^{ref} \mathbf{v} \quad (23)$$

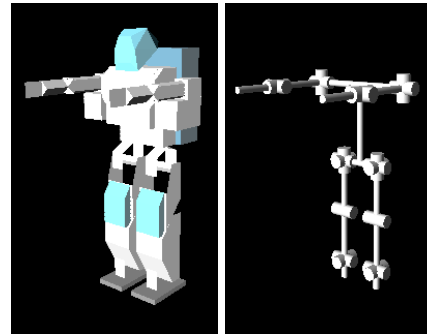
The set of joint torque which makes the joint angles follow ${}^{ref} \dot{\boldsymbol{\theta}}$ is calculated by local feedback controller, such as simple PD control, at each joint.

Fig.4 shows the procedure, where where

$$\mathbf{J}_i {}^{ref} \dot{\boldsymbol{\theta}} = {}^{ref} \mathbf{v}_i \quad (24)$$

is a partial constraint to denote the motion. They are switched in accordance with contact condition and motion scheme. In other words, the motion both in contact and in aerial phase is created only by switching of the constraints and no other procedure. Consequently, the controller stands invariable on contact phase.

4 Simulation



DOF: 20 (8 for arm, 12 for leg)
height: 480 [mm]
weight: 6.5 [kg]

Figure 5: Kinematic structure, size and mass of the robot

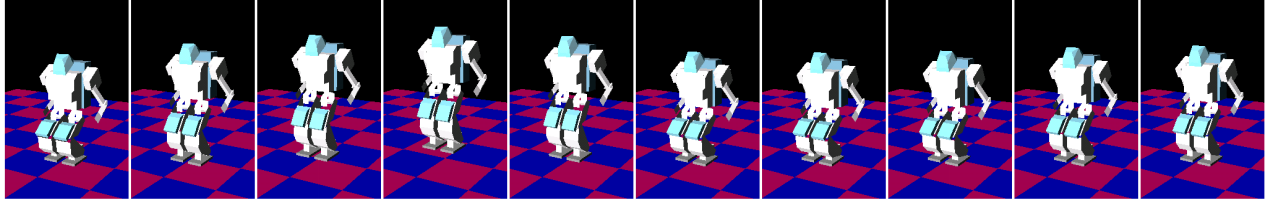


Figure 6: Snapshot of a jumping motion simulation

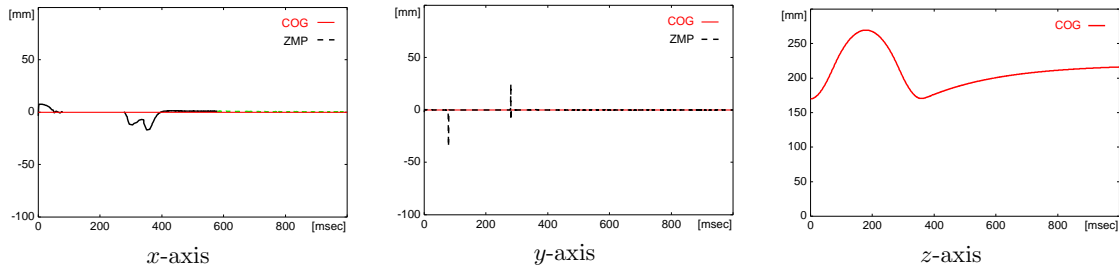


Figure 7: Loci of COG and ZMP in each axis

We realized a jumping motion in computer simulation with the controller proposed, using a robot model of HOAP-1(Fujitsu Automation Ltd.)[18]. Kinematic structure, size and mass of the robot are shown in Fig.5.

The planned maximum stooping depth, height at the detachment-off and the maximum height of jumping were 50[mm],220[mm] and 50[mm] respectively, and the referential height of COG after the touchdown was 220[mm]. Impedance in each phase were decided in accordance with values and equations derived in section 2.2 Fig.6 is a snapshot of the motion. And the loci of COG and ZMP are shown in Fig.7. We can see that the impedance control method works properly and the stable jumping motion is achieved.

5 Conclusion

We introduced Variable Impedant Inverted Pendulum(VIIP) model, augmenting one in [16]. Thanks to it, indirect manipulation of ZMP and vertical reaction force is achieved rather easily, which makes the transition between contact and aerial phase seamless with adequately designed impedance.

Handling of the external force, which generally requires a large amount of computation and is time-consuming, is translated into the COG velocity control equivalently, so that it is time-saving and applicable for realtime implementation.

Another advantage is that it is invariant on contact phase since the COG velocity control is expressed as no more than a part of the constraints which are switched in ac-

cordance with contact phase and motion scheme. The motion both in contact and in aerial phase is realized in the unified way.

Acknowledgment

This research was supported by the “Robot Brain Project” under the Core Research for Evolutional Science and Technology (CREST program) of the Japan Science and Technology Corporation (JST).

References

- [1] Ferdinand Gubina, Hooshang Hemami and Robert B.McGhee. On the Dynamic Stability of Biped Locomotion. *IEEE Transactions on Bio-Medical Engineering*, BME-21(2):102–108, 1974.
- [2] Hirofumi Miura and Isao Shimoyama. Dynamic Walk of a Biped. *The International Journal of Robotics Research*, 3(2):60–74, 1984.
- [3] A.Sano J.Furusho. Sensor-based control of a nine-link biped. *The International Journal of Robotics Research*, 9(2):83–98, 1990.
- [4] S. Kajita and K. Tani. Experimental Study of Biped Dynamic Walking in the Linear Inverted Pendulum Mode. In *Proceedings of the 1995 IEEE International Conference on Robotics & Automation*, pages 2885–2819, 1995.
- [5] Kazuo Hirai, Masato Hirose, Yuji Haikawa and Toru Takenaka. The Development of Honda Humanoid Robot. In *Proceeding of the 1998 IEEE International Conference on Robotics & Automation*, pages 1321–1326, 1998.
- [6] Jin’ichi Yamaguchi, Sadatoshi Inoue, Daisuke Nishino and Atsuo Takanishi. Development of a Bipedal Humanoid Robot Having Antagonistic Driven Joints and Three DOF Trunk. In *Proceedings of the 1998 IEEE/RSJ International Conference on Intelligent Robots and Systems*, pages 96–101, 1998.
- [7] Koichi Nishiwaki, Tomomichi Sugihara, Satoshi Kagami, Masayuki Inaba and Hirochika Inoue. Online Mix-

ture and Connection of Basic Motions for Humanoid Walking Control by Footprint Specification. In *Proceedings of the 2001 IEEE International Conference on Robotics & Automation*, pages 4110–4115, 2001.

[8] Marc H.Raibert. *Legged Robots That Balance*. MIT Press, 1986.

[9] Ken'ichiro Nagasaka. *The Whole-body Motion Generation of Humanoid robot Using Dynamics Filter(Japanese)*. PhD thesis, Univ. of Tokyo, 2000.

[10] Katsu Yamane and Yoshihiko Nakamura. Dynamics Filter — Concept and Implementation of On-Line Motion Generator for Human Figures. In *Proceedings of the 2000 IEEE International Conference on Robotics & Automation*, pages 688–695, 2000.

[11] Shuuji Kajita, Takashi Nagasaki, Kazuhito Yokoi, Kenji Kaneko and Kazuo Tanie. Running Pattern Generation for a Humanoid Robot. In *Proceedings of the 2002 IEEE International Conference on Robotics & Automation*, pages 2755–2761, 2002.

[12] T.Hirano, T.Sueyoshi and A.Kawamura. Development of ROCOS(Robot Control Simulator) - Jump of human-type biped robot by the adaptive impedance control. In *Proceeding of 6th International Workshop on Advanced Motion Control*, 2000.

[13] T.Mita and T.Ikeda. Proposal of a Variable Constraint Control for SMS and Its Application to Running and Jumping Quadruped. In *IEEE International Conference on System, Man and Cybernetics*, 1999.

[14] Keisuke Arikawa and Tsutomu Mita. Design of Multi-DOF Jumping Robot. In *Proceedings of the 2002 IEEE International Conference on Robotics & Automation*, pages 3992–3997, 2002.

[15] F.Pfeiffer, K.Löffler and M.Gienger. The Concept of Jogging JOHNNIE. In *Proceedings of the 2002 IEEE International Conference on Robotics & Automation*, pages 3129–3135, 2002.

[16] Tomomichi Sugihara, Yoshihiko Nakamura, and Hirochika Inoue. Realtime Humanoid Motion Generation through ZMP Manipulation based on Inverted Pendulum Control. In *Proceedings of the 2002 IEEE International Conference on Robotics & Automation*, pages 1404–1409, 2002.

[17] M. Vukobratović and J. Stepanenko. On the Stability of Anthropomorphic Systems. *Mathematical Biosciences*, 15(1):1–37, 1972.

[18] <http://www.automation.fujitsu.com/products/products07.html>(Japanese).

[19] S. Kagami, F. Kanehiro, Y. Tamiya, M. Inaba and H. Inoue. AutoBalancer: An Online Dynamic Balance Compensation Scheme for Humanoid Robots. In *Proceedings of the 4th International Workshop on Algorithmic Foundation on Robotics(WAFR'00)*, 2000.

[20] David E.Orin and William W.Schrader. Efficient Computation of the Jacobian for Robot Manipulators. *The International Journal of Robotics Research*, 3(4):66–75, 1984.

Appendix: COG Jacobian

Since COG \mathbf{p}_G is the function with an argument $\boldsymbol{\theta}$, there is a Jacobian \mathbf{J}_G which relates $\dot{\boldsymbol{\theta}}$ to $\dot{\mathbf{p}}_G$.

$$\dot{\mathbf{p}}_G = \frac{\partial \mathbf{p}_G}{\partial \boldsymbol{\theta}} \dot{\boldsymbol{\theta}} \equiv \mathbf{J}_G \dot{\boldsymbol{\theta}} \quad (25)$$

We call this \mathbf{J}_G *COG Jacobian*.

Hirano et al.[12] introduced the idea of COG Jacobian which were for a simple three-link model. In the case of practical humanoid robots, \mathbf{J}_G is a quite complex non-linear function with multiple arguments. Tamiya et al.[19] proposed the method to calculate it using the numerical quasi-gradient, which needs a large amount of computation and also is less accurate. We developed a fast and accurate calculation method of \mathbf{J}_G with the numerical approach as follows.

Firstly, The relative COG velocity with respect to the total body coordinate(which moves with the base link of the robot together) ${}^0\dot{\mathbf{p}}_G$ can be expressed as

$${}^0\dot{\mathbf{p}}_G = \frac{\sum_{i=0}^{n-1} m_i {}^0\dot{\mathbf{r}}_i}{\sum_{i=0}^{n-1} m_i} = \frac{\sum_{i=0}^{n-1} m_i {}^0\mathbf{J}_{Gi} \dot{\boldsymbol{\theta}}}{\sum_{i=0}^{n-1} m_i} \quad (26)$$

where m_i is the mass of link i , ${}^0\mathbf{r}_i$ is the position of the center of mass of link i with respect to the total body coordinate, and ${}^0\mathbf{J}_{Gi}$ ($3 \times n$) is defined by

$${}^0\mathbf{J}_{Gi} \equiv \frac{\partial {}^0\mathbf{r}_i}{\partial \boldsymbol{\theta}} \quad (27)$$

${}^0\mathbf{J}_G$ is calculated easily by the method proposed by Orin et al.[20]

Therefore, Jacobian ${}^0\mathbf{J}_G$ which relates $\dot{\boldsymbol{\theta}}$ to ${}^0\dot{\mathbf{p}}_G$ is

$${}^0\mathbf{J}_G = \frac{\sum_{i=0}^{n-1} m_i {}^0\mathbf{J}_{Gi}}{\sum_{i=0}^{n-1} m_i} \quad (28)$$

Secondly, suppose link F is at rest in the inertia frame, as the foot link of the supporting leg for instance, the linear and angular velocity of the base link with respect to the world coordinate, $\dot{\mathbf{p}}_0$ and $\boldsymbol{\omega}_0$, are available from

$$\boldsymbol{\omega}_0 = -\mathbf{J}_{\omega F} \dot{\boldsymbol{\theta}} \quad (29)$$

$$\begin{aligned} \dot{\mathbf{p}}_0 &= -\boldsymbol{\omega}_0 \times \mathbf{R}_0 {}^0\mathbf{p}_F - \mathbf{R}_0 {}^0\dot{\mathbf{p}}_F \\ &= \mathbf{R}_0 (-{}^0\boldsymbol{\omega}_F \times {}^0\mathbf{p}_F - {}^0\mathbf{J}_F \dot{\boldsymbol{\theta}}) \end{aligned} \quad (30)$$

where \mathbf{R}_0 is the attitude matrix of the base link with respect to the world coordinate, ${}^0\mathbf{p}_F$ is the position of the link F in the total body coordinate, ${}^0\boldsymbol{\omega}_F$ is the relative rotation velocity of the link F with respect to the total body coordinate, ${}^0\mathbf{J}_F$ and ${}^0\mathbf{J}_{\omega F}$ are the Jacobian about relative linear and angular velocity of the link F with respect to the total body coordinate, and the notation $[\mathbf{v}^\times]$ means outer-product matrix of a vector \mathbf{v} (3×1).

Then, the COG velocity with respect to the world coordinate $\dot{\mathbf{p}}_G$ is

$$\begin{aligned} \dot{\mathbf{p}}_G &= \dot{\mathbf{p}}_0 + \boldsymbol{\omega}_0 \times \mathbf{R}_0 {}^0\mathbf{p}_G + \mathbf{R}_0 {}^0\dot{\mathbf{p}}_G \\ &= \mathbf{R}_0 \{ {}^0\dot{\mathbf{p}}_G - {}^0\dot{\mathbf{p}}_F + ({}^0\mathbf{p}_G - {}^0\mathbf{p}_F) \times {}^0\boldsymbol{\omega}_F \} \\ &= \mathbf{R}_0 \{ {}^0\mathbf{J}_G - {}^0\mathbf{J}_F + [({}^0\mathbf{p}_G - {}^0\mathbf{p}_F)^\times] {}^0\mathbf{J}_{\omega F} \} \dot{\boldsymbol{\theta}} \end{aligned} \quad (31)$$

And we can conclude that \mathbf{J}_G is

$$\mathbf{J}_G = \mathbf{R}_0 \{ {}^0\mathbf{J}_G - {}^0\mathbf{J}_F + [({}^0\mathbf{p}_G - {}^0\mathbf{p}_F)^\times] {}^0\mathbf{J}_{\omega F} \} \quad (32)$$